Collision induced absorption spectra and line broadening of CsRg system (Rg=Xe, Kr, Ar, Ne) studied by the symmetry adapted cluster-configuration interaction (SAC-CI) method

Masahiro Ehara and Hiroshi Nakatsuji
Department of Synthetic Chemistry and Biological Chemistry, Faculty of Engineering, Kyoto University, Kyoto 606, Japan and Institute for Fundamental Chemistry, 34-4, Takano-Nishihiraki-cho, Sakyou-ku, Kyoto 606, Japan

(Received 29 August 1994; accepted 27 January 1995)

The collisionally induced absorption process and the broadening of the $6P$ resonance line of the Cs–Rg system (Rg=Xe, Kr, Ar, and Ne) are studied theoretically by the symmetry adapted cluster-configuration interaction (SAC-CI) method. The potential energy curves and the transition moments of the CsRg system correlating to the $6S$, $6P$, $5D$, and $7S$ states of the Cs atom are investigated. The reduced absorption coefficients are calculated using the quasistatic approximation and the results agree well with the experimental data. The monotonic dependence of the spectral peaks on the rare gas species is due to the similar monotonic dependence of the avoided crossing point between the $7s\Sigma$ and $5d\Sigma$ states. The absorption intensities decrease as the rare gas atom is substituted from Xe to Ne in agreement with the experimental observation. The intensities of the $6s\Sigma-5d\Sigma$ transitions are calculated to be larger than those of the $6s\Sigma-7s\Sigma$ ones, since the former transitions are induced at larger internuclear distances than the latter. © *1995 American Institute of Physics.*

I. INTRODUCTION

Chemical reactions in optical fields have received much attention in recent years in the field of spectroscopy.[1] Collision induced dipole transitions and line broadening contain important information on the interaction potentials of the ground and excited states and the collisional dynamics of the transient species, and have been widely observed and investigated for alkali atoms[2–11] and alkali–earth atoms[12–15] perturbed by rare gas atoms. In particular, the Cs–rare gas (Cs–Rg) system shows relatively strong interactions and therefore, its absorption and/or emission spectra exhibit large intensity, shifts, broadening, and asymmetry. The dipole forbidden transitions, the $S-S$ and $S-D$ transitions, of the Cs atom are induced by the collisions with the rare gas atoms,[2,3] these collision induced absorption spectra were observed by Moe *et al.*[2] The broadening and the shift of the resonance lines have also been observed for this system; Hedges *et al.*[5] and Kielkopf *et al.*[6] reported the detailed spectra for the $6S-6P$ emissions and $6S-nP$ absorptions of the Cs atom.

Several theoretical studies have been performed to elucidate the mechanisms of the collision induced transitions and the line broadening.[7–10] Baylis[7] investigated the line broadening of the $6S-6P$ transitions of the alkali–rare gas systems employing the semiempirical potential curves. Pascale *et al.* calculated the potential energy curves[8] and the oscillator strengths[9] of the alkali-rare gas systems using the semiempirical model of Baylis[7] and investigated their collision induced absorption processes. However, because of the limitations in their procedure, they could not reproduce well the experimental spectra for the Cs–Rg system.[10]

In a previous paper, we investigated the collision induced absorption process of the Cs–Xe system using the *ab initio* symmetry adapted cluster-configuration interaction (SAC-CI) method for including electron correlations.[11] However, the ordering of the $5D$ and $7S$ levels of the Cs atom was not properly reproduced in that calculation. In the present study, we have overcome this problem by using refined basis sets. We are interested in the interatomic interactions at intermediate region, which are related to the far-wing regions of the spectra. The SAC/SAC-CI method[16–18] is used for the calculations of the van der Waals (vdw) interactions of the open-shell Cs–Rg system. The method has been applied successfully to a large number of molecular spectroscopy problems,[18] including the diatomic systems like Li_2 (Ref. 19) and Ar_2.[20] The reduced absorption coefficient, which is directly determined by experiment, is estimated by the quasistatic approximation.[5,21–23]

II. CALCULATIONAL DETAILS

The basis sets should be flexible enough to describe the vdw interactions. In the previous study,[11] we used for Cs the relativistic effective core potential of Hay and Wadt[24] and the diffuse functions proposed by Langhoff *et al.*[25] However, we failed to reproduce the proper energy ordering of the $5D$ and $7S$ states of the Cs atom, even though the core polarization effects were included. The relative positions and the interactions of these states in the Cs–Rg systems are quite important for reproducing the spectra and therefore, we first examine here the all-electron basis of Huzinaga *et al.*[26] The excitation energies calculated at almost the dissociation limit of the systems (15.0 Å) using the Huzinaga basis are given in Table I and compared with the previous results in Fig. 1. The deviations of the present results from the experimental values are within 0.25 eV and the ordering of the excited states of the Cs atom is properly reproduced. The f-functions are not important for the excitation energy and therefore, are not included in the present study.

We thus use the Huzinaga basis set[26] and all electrons are explicitly treated for both the Cs and Rg atoms. The basis set of Cs is composed of $[7s5p2d]$ set for the valence part,

 0021-9606/95/102(17)/6822/9/$6.00

TABLE I. Excitation energy of the Cs atom (eV).

State	Expt[a]	SAC-CI[b]
$6P(^2P_{1/2}, {}^2P_{3/2})$	1.386, 1.455	1.18
$5D(^2D_{3/2}, {}^2D_{5/2})$	1.798, 1.810	1.78
$7S(^2S_{1/2})$	2.298	2.04
$7P(^2P_{1/2}, {}^2P_{3/2})$	2.699, 2.721	2.68
$6D(^2D_{3/2}, {}^2D_{5/2})$	2.800, 2.806	2.70

[a]Reference 32; the splittings are due to the spin–orbit interaction.
[b]Calculated using the Huzinaga's basis set for CsRg at the internuclear distance of 15.0 Å.

augmented with the $(3s3p3d)$ primitive sets of Langhoff *et al.*[25] for the Rydberg states. The Xe basis is the $[6s5p2d]$ set plus $(2d)$ polarization functions of Huzinaga[26] augmented with the primitives $(3s2p)$ of Ermler *et al.*[27] The basis sets of the other rare gas atoms are of similar quality to that of Xe; namely, the Rg basis set is derived from $[ns(n-1)p(n-4)d]$ $[n=5(\mathrm{Kr}),\ n=4(\mathrm{Ar}),$ and $n=3(\mathrm{Ne};3s2p)]$ plus polarization $(2d)$ set of Huzinaga[26] augmented with the diffuse $(2s2p)$ functions. The final set is $[10s8p5d]/[ns(n-1)p(n-4)d]$ for CsRg $[n=8(\mathrm{Xe}),\ n=7(\mathrm{Kr}),\ n=6(\mathrm{Ar}),$ and $n=5(\mathrm{Ne};5s4p2d)]$. The resultant SCF dimensions are 117, 107, 97, and 93 for CsXe, CsKr, CsAr, and CsNe, respectively. Relativistic effects are not included in the present study. Calculations are performed at 13 Cs–Rg distances from 3 to 15 Å.

The SAC-CI method[17] is used for calculating correlated wave functions. Details of the SAC (Ref. 16) and SAC-CI (Ref. 17) theories have been reported elsewhere.[18] For CsXe, the cation $CsXe^+$ is solved by the SAC method and the various states of CsXe are constructed by the SAC-CI method. The eight occupied valence MO's $(5s_{Xe}5p_{Xe}5s_{Cs}5p_{Cs}6s_{Cs})$ and the lower 41 unoccupied MO's are adopted for the active space. In the SAC step, configuration selection[28] is performed with the threshold of $\lambda_g=1\times10^{-5}$ a.u. for the linked operators. In the SAC-CI step, no configuration selection is performed for the linked terms, because weak interactions of the vdw system should be calculated. The resulting SAC-CI dimensions are 3961(Σ states), 3370(Π states), and 2788(Δ states) for all the internuclear distances. For the other CsRg systems, the calculations are of similar accuracy to those of the CsXe system. The SCF orbitals were calculated using the program HONDO7 (Ref. 29) and the SAC/SAC-CI calculations were performed using the program SAC85.[30]

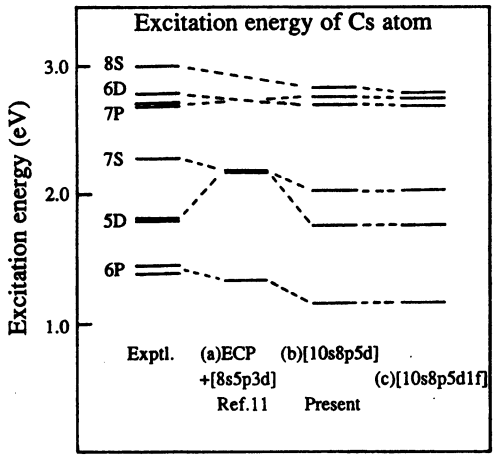

FIG. 1. Basis set dependence of the excitation energy of the Cs atom; (a) basis set used in Ref. 11; (b) basis set used in the present study; and (c) basis set (b) plus f-function proposed in Ref. 25.

To investigate the fine structures observed for the $6P$ state, the spin–orbit interactions are included by the method reported earlier.[31] The spin–orbit coupling constant is estimated to be $\zeta p=369.4\ \mathrm{cm}^{-1}$ from the atomic spectral data.[32]

The basis set superposition error (BSSE) is taken into account. The BSSE of atom A is calculated as

$$\delta_A=E_A(\phi_A\cup\phi_B)-E_A(\phi_A), \tag{1}$$

where ϕ_A and ϕ_B denote the basis sets centered at A and B, respectively. The total BSSE correction is estimated as

$$\delta=\delta_A+\delta_B. \tag{2}$$

The BSSE of the excited states is assumed to be the same as that of the ground state.

The quasistatic approximation[5,21–23] is adopted for calculating the reduced absorption coefficient. Though there exist more elaborate treatments,[33] this approximation seems to be reliable and also useful for understanding the mechanism of the collision induced absorption process. Assuming a binary collision between Cs and Rg atoms in the canonical distribution, the reduced absorption coefficient is given by[23]

$$\frac{k(\lambda)}{n_G n_A}=\sum_c \frac{4\pi^3}{3\lambda} D(R_c)^2\left\{\frac{4\pi R_c^2}{d[V_e(R)-V_g(R)]/dR|_{R_c}}\right\} \times\exp\left[-\frac{V_g(R_c)-V_g(\infty)}{k_BT}\right], \tag{3}$$

where n_G and n_A are the densities of the perturber Rg and the absorber Cs, respectively, $D(R)$ denotes the induced transition dipole moment at internuclear distance R, and V_g and V_e are the energies of the ground and excited states, respectively.

III. POTENTIAL ENERGY CURVES

We have calculated the ground and excited states of the Cs–Rg system correlating to the $6S$ (ground), $6P$, $5D$, and $7S$ states of the Cs atom. Though the excitations to the $5D$ and $7S$ states are originally dipole forbidden, they are collisionally induced through the interaction with the rare gas atom. For the dipole-allowed $6S-6P$ transition, collisional perturbations by rare gas atoms lead to the broadening of the resonance line.

First, the potential curves of the CsXe system are given; those of the other CsRg systems are similar. Figure 2 shows the calculated potential curves of the $6S$, $6P$, $5D$, and $7S$ states of CsXe. Hund's case a, which is suitable for describing the present system,[2] is adopted. The calculated spectroscopic constants for the bound states of the CsRg system are summarized in Table II.

The calculated potential curve of the ground state of CsXe has a flat shape with a shallow minimum of 30 cm^{-1} at

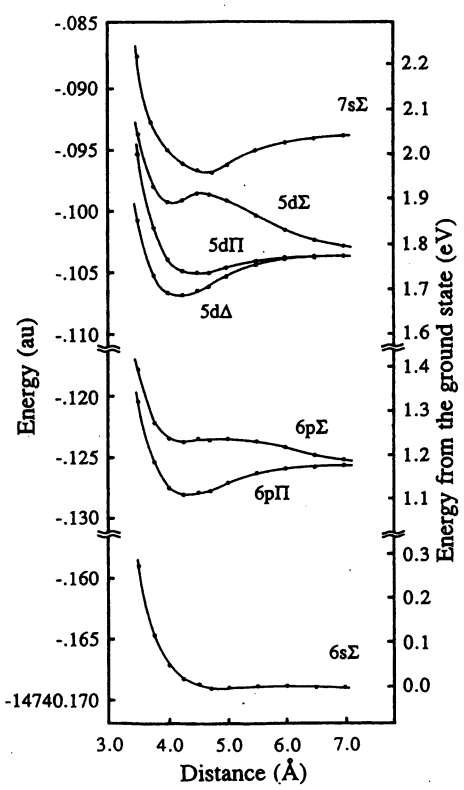

FIG. 2. Potential energy curves of the $6s$, $6p$, $5d$, and $7s$ states of the CsXe system without spin–orbit coupling.

4.97 Å, while in the atomic scattering experiment of Buck and Pauly, a well of 110 cm^{-1} is observed at 5.45 Å.[34] For the other complexes, no potential minima were calculated for the ground states after considering the BSSE, though shallow wells were observed experimentally for the ground states of CsKr and CsAr.[34]

The $6p\Sigma$ and $5d\Sigma$ states are due to the excitations from the $6s$ nonbonding MO to the weakly antibonding $6p\sigma$ and $5d\sigma$ MO's, so that the system becomes unstable and the potential curves are repulsive. The repulsive interaction in the $5d\Sigma$ state seems to be larger than that in the $6p\Sigma$ state and starts from a larger internuclear distance. The $5d\Sigma$ state has a characteristic hump at 4.6 Å and the $6p\Sigma$ state has a shoulder at 5.0 Å. These features were also obtained in the semiempirical calculation.[8] The hump of the $5d\Sigma$ state is caused by an avoided crossing with the $7s\Sigma$ state so that the natures of these states are reversed at this point, though in Fig. 2 the upper curve is still called the $7s\Sigma$ state and the lower one the $5d\Sigma$ state even in the shorter region. Pascale *et al.*[8] explained that the hump in the $6p\Sigma$ state occurs through the interaction with the neighboring states of the same symmetry corresponding to $5D_{3/2}$ and $5D_{5/2}$ levels in their dissociation limits. We also observe a configuration mixing with the $6s\rightarrow 5d\sigma$ component in the $6p\Sigma$ state, which may cause the shoulder in the potential curve.

The $6p\Pi$, $5d\Pi$, and $5d\Delta$ states have shallow minima in their potential curves. The Rydberg orbitals of these states of the Cs atom are not directed towards the rare gas atom, but the ion core of the Cs atom polarizes the electron density of the rare gas atom, which is responsible for the attractive force. For CsXe, the dissociation energy and the equilibrium distance are calculated to be D_e=538 cm^{-1} and R_e=4.33 Å for $6p\Pi$, D_e=280 cm^{-1} and R_e=4.48 Å for $5d\Pi$, and D_e=698 cm^{-1} and R_e=4.20 Å for $5d\Delta$, as shown in Table II. Since the Rydberg orbital of the $5d\Pi$ state has a component along the CsRg axis, the attractive force is smaller than those in the $6p\Pi$ and $5d\Delta$ states. Therefore, the equilibrium distance, R_e, of the $5d\Pi$ state is calculated to be larger than those of the $6p\Pi$ and $5d\Delta$ states and the binding energy, D_e, of the former is smaller. The potential curve of the $7s\Sigma$ state also has a well (662 cm^{-1}) at 4.61 Å which is due to the avoided crossing with the $5d\Sigma$ state, as noted above.

The potential energy curves of the $5d\Sigma$, $5d\Pi$, $5d\Delta$, and $7s\Sigma$ states of CsRg (Rg=Xe, Kr, Ar, and Ne) are compared in Fig. 3. The attractive wells of the $5d\Pi$, $5d\Delta$, and $7s\Sigma$ states become shallower and the equilibrium distances become shorter as the rare gas atom is replaced from Xe to

TABLE II. Calculated spectroscopic constants for the bound states of the CsRg (Rg=Xe, Kr, Ar) system.

System	State	Expt. D_e (cm^{-1})	SAC-CI D_e(cm^{-1})	SAC-CI R_e (Å)	SAC-CI ω_e (cm^{-1})
CsXe	$6s\Sigma$ (Ground)	110[a]	30	4.97	···
	$5d\Delta$		698	4.20	33.2
	$5d\Pi$		280	4.48	23.5
	$7s\Sigma$	~890[b]	662	4.61	33.8
	$6p^2\Pi_{1/2}$	~430[c]	425	4.27	32.5
	$6p^2\Pi_{3/2}$	~500[c]	538	4.33	32.4
CsKr	$5d\Delta$		441	3.90	46.2
	$7s\Sigma$		322	4.35	22.3
	$6p^2\Pi_{1/2}$	~300[c]	163	3.95	35.1
	$6p^2\Pi_{3/2}$	~350[c]	283	3.98	38.3
CsAr	$5d\Delta$		340	3.69	···
	$7s\Sigma$		113	4.27	···

[a]Reference 34.
[b]Reference 2.
[c]Reference 5.

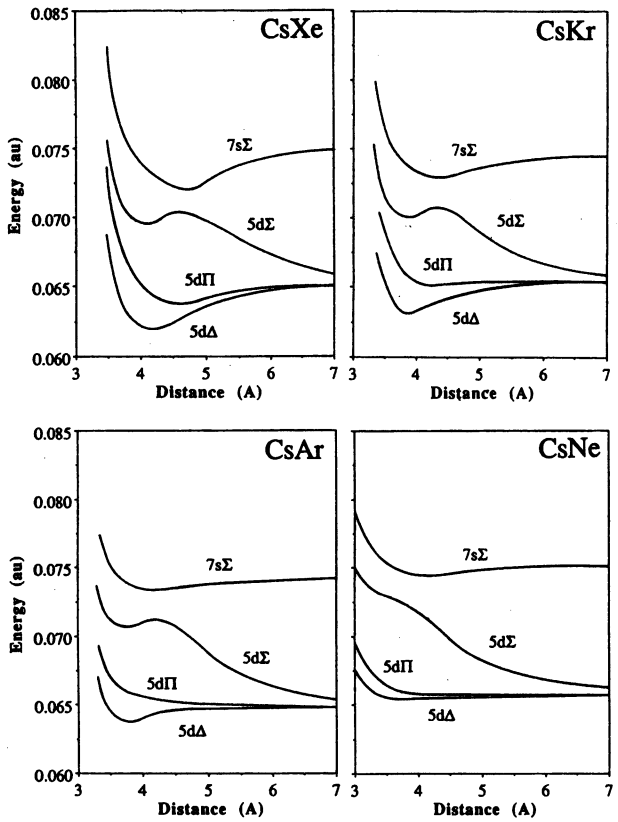

FIG. 3. Potential energy curves of the $5d\Sigma$, $5d\Pi$, $5d\Delta$, and $7s\Sigma$ states of the CsRg system (Rg=Xe, Kr, Ar, and Ne). Energy is relative to the dissociation limit of the ground states.

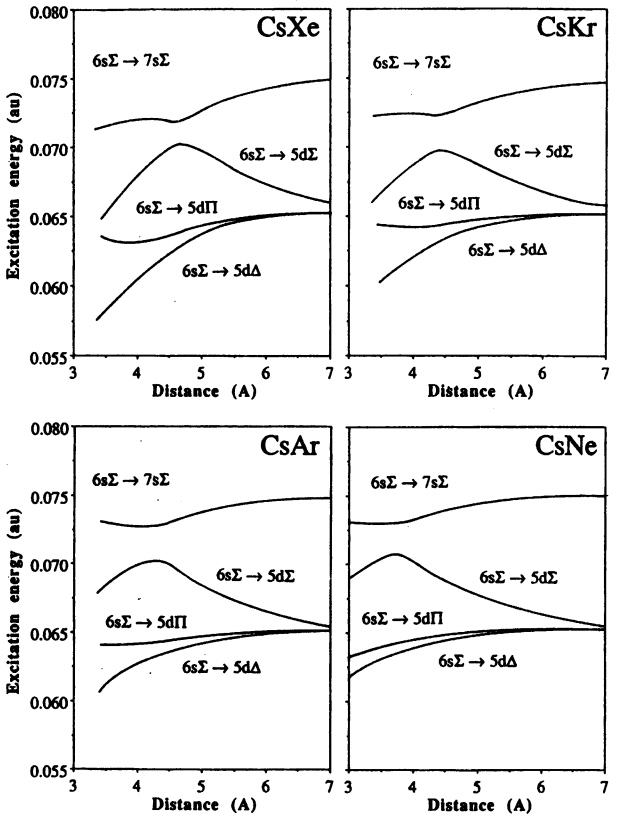

FIG. 4. Excitation energy as a function of the internuclear distance (difference potential) of the $5d\Sigma$, $5d\Pi$, $5d\Delta$, and $7s\Sigma$ states of the CsRg system (Rg=Xe, Kr, Ar, and Ne).

Ne. For example, the dissociation energies and equilibrium distances of the $5d\Delta$ and $7s\Sigma$ states of CsKr are calculated to be 441 cm^{-1} at 3.90 Å and 332 cm^{-1} at 4.35 Å, respectively, and the $5d\Pi$ state is almost flat. These features are clearly explained in terms of the polarizability and the vdw radius of the rare gas atom. According to these changes, the avoided crossing between the $5d\Sigma$ and $7s\Sigma$ states occurs at shorter internuclear distances as the rare gas atom is substituted from Xe to Ne. The avoided crossing points are calculated to be around 4.6 Å, 4.3 Å, and 4.1 Å for CsXe, CsKr, and CsAr, respectively. Correspondingly, the observed peaks of the collision induced absorptions show monotonic shifts; namely, the $6s\Sigma \rightarrow 7s\Sigma$ peak becomes closer to the free atomic position (Fig. 7) and the $6s\Sigma \rightarrow 5d\Sigma$ peak becomes more distant from the free atomic position (Fig. 8), as the rare gas atom is replaced from Xe to Ne. Thus, the monotonic shift of the collision induced absorption peaks with substituting rare gas atom is confirmed to be due to the change in the relative position of the avoided crossing point.

Figure 4 shows the difference potential, which is the dependence of the excitation energy on the internuclear distance, for the $5d\Sigma$, $5d\Pi$, $5d\Delta$, and $7s\Sigma$ states. The difference potential gives the absorption energy at the corresponding nuclear distance. It is clear that the $5d\Sigma$ states are responsible for the absorption bands on the blue side of the atomic forbidden line, while the $7s\Sigma$ and $5d\Pi$ states give rise to those on the red side. The $6s\Sigma \rightarrow 5d\Delta$ transition is forbidden even in the collision system as shown in the next section. The difference potentials for the $6s\Sigma - 5d\Sigma$ transitions have extrema at 4.69, 4.39, 4.19, and 3.68 Å for CsXe, CsKr, CsAr, and CsNe, respectively. These values reflect the positions of the hump in the $5d\Sigma$ states caused by the avoided crossing between the $5d\Sigma$ and $7s\Sigma$ states. The semiempirical calculation also gives the extremum at 4.34 Å for CsXe.[8] On the other hand, the excitation energies of the $7s\Sigma$ and $5d\Pi$ states decrease with the internuclear distance and there exist a flat region at small distances. This existence of the flat region supports the interpretation of the experimental $6s\Sigma - 7s\Sigma$ absorption spectra due to Moe *et al.*[2] as discussed in Sec. V. In a classical picture, these extrema and flat regions in the difference potentials correspond to the peaks of the shifted bands, as seen from Eq. (3). Tables III

TABLE III. Energy shift of the $6s\Sigma - 7s\Sigma$ excitation of the CsRg system relative to the $6S-7S$ transition of the Cs atom (in cm^{-1}).

System	Expt[a]	SAC-CI[b]	PV[c]
CsXe	−1061	−630	−136
CsKr	−829	−480	−676
CsAr	−741	−420	···
CsNe	−500	−370	217

[a]Reference 2.
[b]Energy shift is estimated from the flat region of the difference potential.
[c]Semiempirical calculation of Ref. 8.

TABLE IV. Energy shift of the $6s\Sigma-5d\Sigma$ excitation of the CsRg system relative to the $6S-5D$ transition of the Cs atom.

System	Expt (cm^{-1})[a]	SAC-CI[b] Shift (cm^{-1})	SAC-CI[b] Internuclear distance (Å)	PV (cm^{-1})[c]
CsXe	1082	1130	4.69	3153
CsKr	1204	1030	4.39	2696
CsAr	1478	1100	4.19	1759
CsNe	1585	1150	3.68	3378

[a]Reference 2.
[b]Energy shift is estimated from the extremum of the difference potential.
[c]Semiempirical calculation of Ref. 8.

and IV give the frequency shifts of the peaks associated to the $7S$ and $5D$ lines, respectively. The shift values are discussed in detail in Sec. V.

IV. TRANSITION MOMENTS

The $6S\rightarrow5D$ and $6S\rightarrow7S$ transitions of the Cs atom are dipole forbidden, but are induced by the interactions with the Rg atoms. The absolute values of the induced dipole moments are shown in Fig. 5 as a function of the internuclear distance. These induced moments are mainly due to the intra-atomic orbital mixing of the p-components of the Cs atom, caused by reduction of the spatial symmetry of the system. Transitions from $6s\Sigma$ to $7s\Sigma$, $5d\Sigma$, and $5d\Pi$ are induced at the nuclear distances from 3 to 7 Å. The $5d\Delta$ state does not have an induced transition dipole moment, and therefore gives no contribution to the induced absorption spectra.

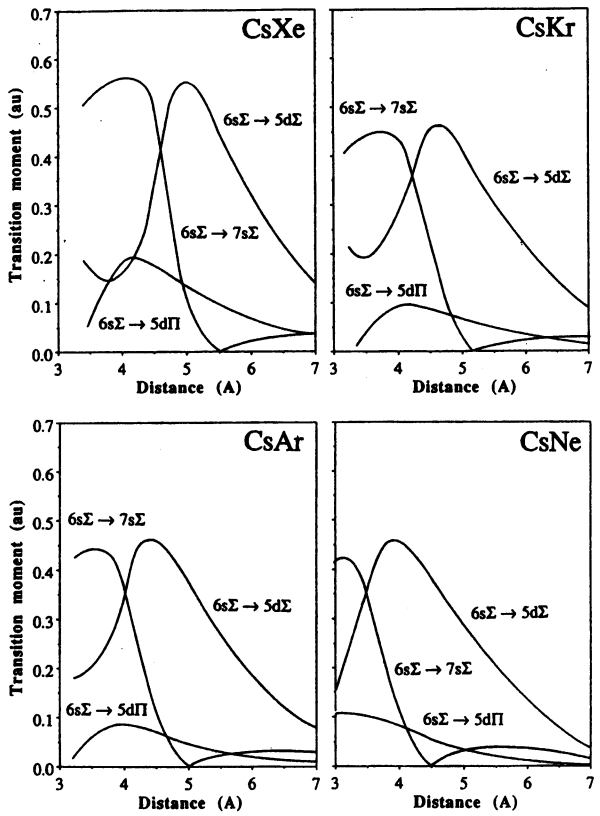

FIG. 5. Absolute value of the transition dipole moments for the $6s\Sigma\rightarrow5d\Sigma$, $6s\Sigma\rightarrow5d\Pi$, and $6s\Sigma\rightarrow7s\Sigma$ excitations of the CsRg system (Rg=Xe, Kr, Ar, and Ne).

The induced transition moment is an important factor, as seen from Eq. (3), in determining the intensity of the induced absorption. The overall behaviors of these transition moments are common to all the CsRg systems. The $6s\Sigma-5d\Sigma$ transition moment is induced at larger internuclear distances than that of $6s\Sigma-7s\Sigma$; the p-component of the Cs atom interacts more readily in the $5d\Sigma$ state than in the $7s\Sigma$ state. Since the Boltzmann factor of the ground state sharply decreases in the repulsive region, $R\lesssim4$ Å, this explains the observation that the reduced absorption coefficients of $6s\Sigma-5d\Sigma$ are larger than those of $6s\Sigma-7s\Sigma$.[1] The magnitude of the transition moment is reversed between the $5d\Sigma$ and $7s\Sigma$ states at the avoided crossing. The $6s\Sigma-7s\Sigma$ transition moment shows an oscillatory structure, as in the semiempirical calculation of Pascale,[9] reflecting the nodal property of the p-component mixed into the $7s\Sigma$ state. Due to this nodal property, the CsXe interaction at around 5–6 Å has only a small contribution to the collision induced absorption around the $7S$ line. The calculated transition moments seem to be underestimated in comparison with the experimental results as discussed below.

V. ABSORPTION SPECTRA

The collision induced absorption spectra are calculated using the quasistatic approximation given by Eq. (3). The $7s$ and $5d$ lines of the CsXe absorption spectra are shown in Fig. 6. In the spectra, the internuclear distance of the collisional complex at which the corresponding energy absorption occurs in a classical picture, is given. It is clearly seen that the vdw complexes at internuclear distances ranging from 3 to 7 Å are the main contributors to the collision induced absorptions.

The experimental and theoretical absorption spectra of the $7S$ band of the CsRg system are compared in Fig. 7. The experimental absorption spectra have broad continuous bands located to the red side of the atomic forbidden line. The energy shift of the peak maximum and the band intensity becomes smaller as the rare gas is substituted from Xe to Ne. The experimental absorption bands have vibrational structures, which indicate the existence of attractive wells in the excited states. As shown in Table II, the calculated $7s\Sigma$ potential curves have attractive wells with the dissociation energies of D_e=662, 322, and 113 cm^{-1} for CsXe, CsKr, and CsAr, respectively, in the order of the polarizabilities of the rare gas atoms. Moe *et al.* proposed[2] a potential well depth of ~890 cm^{-1} for the $7s\Sigma$ state of CsXe through the analysis of the absorption spectrum. They also reported[2] that the spectral shapes and the peak shifts do not change with varying temperature, therefore this red-shifted band occurs by a mechanism similar to that of the satellite observed for the dipole-allowed transition.

Accordingly, there exist flat regions in the difference potentials of the $6s\Sigma-7s\Sigma$ transitions for all the species, as noted previously. The classical treatment breaks down for these regions and the calculated absorption intensities diverge to infinity at the corresponding energies. The energy

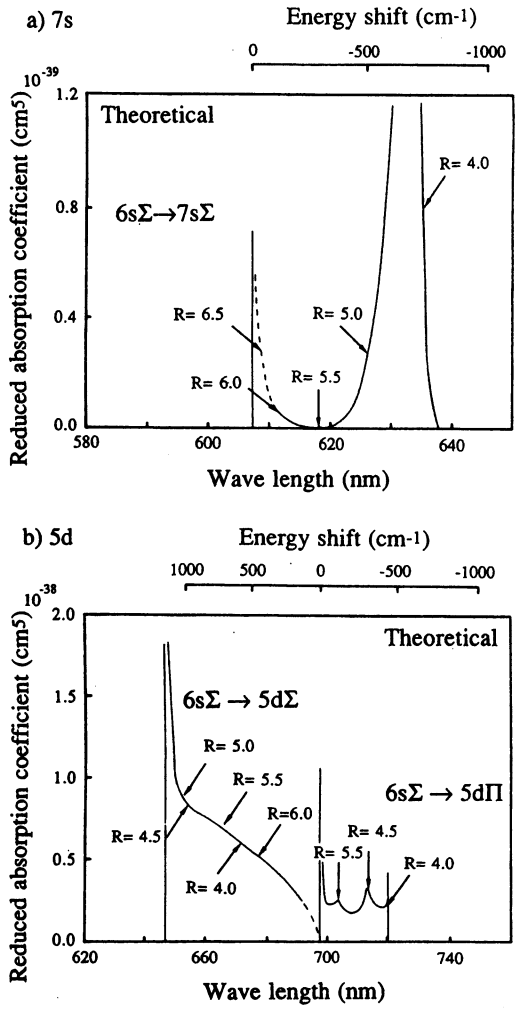

FIG. 6. Calculated collision induced absorption spectra for (a) $7s$ and (b) $5d$ states of the Cs–Xe system. Values in the spectra show the internuclear distance at which the corresponding transition occurs in a classical picture.

shifts from the Cs atomic forbidden $6S-7S$ peak are given in Table III. The red shifts of $6s\Sigma-7s\Sigma$ are calculated to be -630 cm^{-1}, -480 cm^{-1}, -420 cm^{-1}, and -370 cm^{-1} for CsXe, CsKr, CsAr, and CsNe, respectively, which reproduces the monotonic change of the peak shift observed in the experiment, though the absolute value are underestimated. The semiempirical calculations did not reproduce this order.[9] Our calculated absorption intensities also reproduce the experimental trends; the absorption intensities decrease as the rare gas is substituted from Xe to Ne.

In Fig. 8, we compare the experimental and theoretical collision induced absorption spectra associated with the $6S-5D$ forbidden transition. The absorption band of the $6S-5D$ transition has a more complex shape than the $6S-7S$ one. This is because the $5d\Sigma$ and $5d\Pi$ states contribute to the induced absorption. The $5d\Sigma$ state is the source of the band in the blue side region of the atomic transition, while the $5d\Pi$ state is responsible for the band in the red side region.

The peak shift of the blue side band of the atomic transition becomes larger, while the intensity of the band becomes smaller, as the rare gas atom is substituted from Xe to Ne. As shown in Fig. 5, the difference potential of the $6s\Sigma-5d\Sigma$ excitation has an extremum for all species. The calculated energy shifts for the $6s\Sigma-5d\Sigma$ excitations are compared in Table IV with the experimental values and with those calculated by Pascale *et al.*[8] The peak shift for CsXe is calculated to be 1130 cm^{-1}, compared to the experimental value of 1082 cm^{-1}. The calculated peak shifts for $6s\Sigma-5d\Sigma$ do not reproduce the experimental ordering with the substitution of the rare gas atom. This is because the energy separation between the $5D$ and $7S$ states of the Cs atom is underestimated in the present calculation.

The $6s\Sigma-5d\Pi$ excitation also has an induced transition dipole moment. This transition is calculated to have smaller intensity in comparison with the $6s\Sigma-5d\Sigma$ excitation and to be located to the red side of the forbidden atomic line. In the experimental spectra[2] the intensity of the absorption band on the red side of the atomic line seems to decrease gradually as the rare gas is substituted from Xe to Ne. On the other hand, the calculated difference potentials have flat regions as shown in Fig. 4, and therefore, the theoretical spectra have limits in their red shifted bands. However, it was noted that the precise experimental analysis of this region was difficult since this band partially overlaps with the absorption band of Cs_2.[2]

VI. BROADENING OF THE 6P EMISSION LINE

The broadening of the $6P$ resonance line is due to the $6p\Sigma$ and $6p\Pi$ states of the CsRg system. Hedges *et al.*[5] analyzed the far wing regions of the emission spectra of the $6P$ line and determined the $A\Pi_{1/2}$, $A\Pi_{3/2}$, $B\Sigma_{1/2}$ potentials of the CsRg system using the quasistatic approximation. An elaborate theoretical study on the far-wing line shape is given by Ma and Tripping.[35]

Figure 9 gives the calculated potential curves of the $6p^2\Sigma_{1/2}$, $6p^2\Pi_{1/2}$, and $6p^2\Pi_{3/2}$ states of the CsXe system including the spin–orbit effects. For the CsXe system, our potential curves of the $6p^2\Pi_{1/2}$ and $6p^2\Pi_{3/2}$ states show good agreement with those experimentally determined by Hedges *et al.*[5] The dissociation energies and the equilibrium distances are calculated to be D_e=425 cm^{-1}, R_e=4.27 Å and D_e=538 cm^{-1}, R_e=4.33 Å for the $6p^2\Pi_{1/2}$ and $6p^2\Pi_{3/2}$ states, respectively, in comparison to the experimental values of D_e=~430 cm^{-1} and D_e=~500 cm^{-1}, respectively.[5] For CsKr, these states are calculated to have shallow potential wells of D_e=163 cm^{-1} and D_e=283 cm^{-1} which compare with the experimental results of D_e=~300 cm^{-1} and D_e=~350 cm^{-1}.[5] The calculated potential curve of the $6p^2\Sigma_{1/2}$ state has a small hump at R_{hump}=5.1 Å (CsXe), which is also reported in the theoretical work of Pascale *et al.*[8] However, the potential curve determined by experiment does not exhibit such a feature.[5]

The calculated and experimental emission spectra for the $6P-6S$ line of the CsXe system are compared in Fig. 10. The difference potential for $6s\Sigma-6p^2\Sigma_{1/2}$ also has an extremum like that of $6s\Sigma-5d\Sigma$ and therefore, the calculated emission band shows a divergence on the blue side. Correspondingly, the experimental spectrum also has a peak of the emission band in the blue region. The calculated shift values and the internuclear distances giving the peaks for the

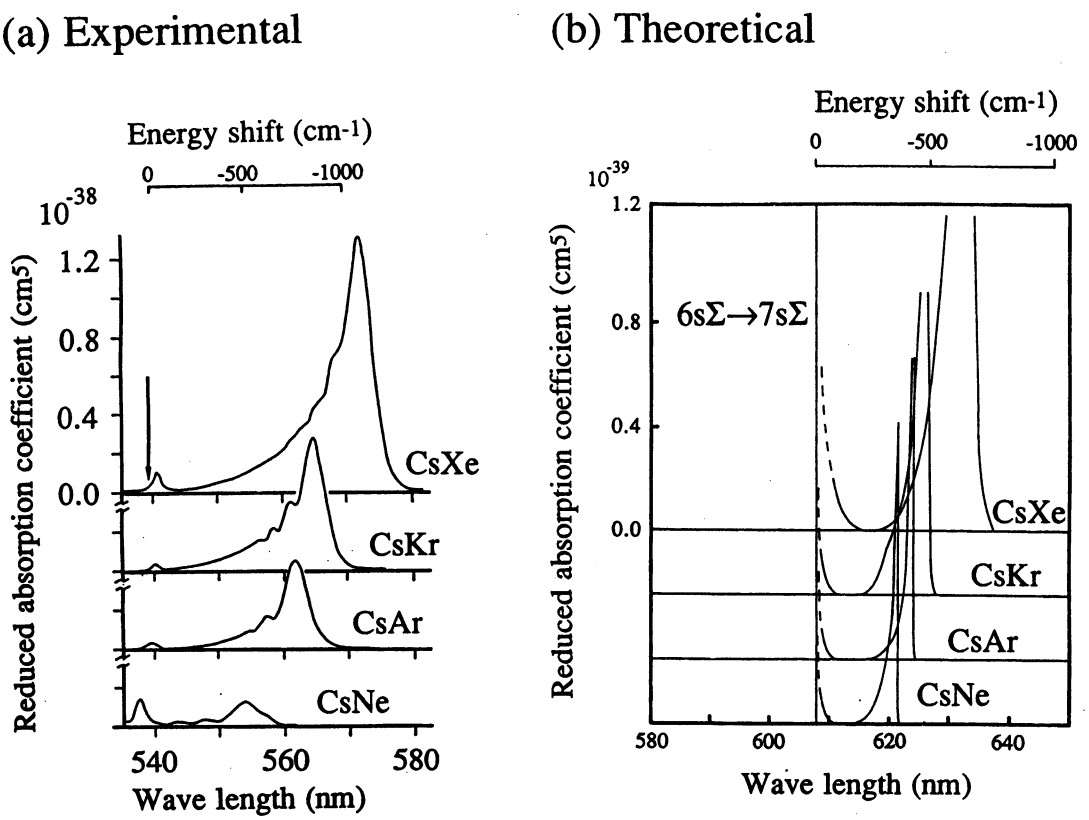

FIG. 7. (a) Experimental and (b) theoretical collision induced absorption spectra for the 7*s* state of the Cs–Rg system. Experimental spectra are cited from Ref. 2.

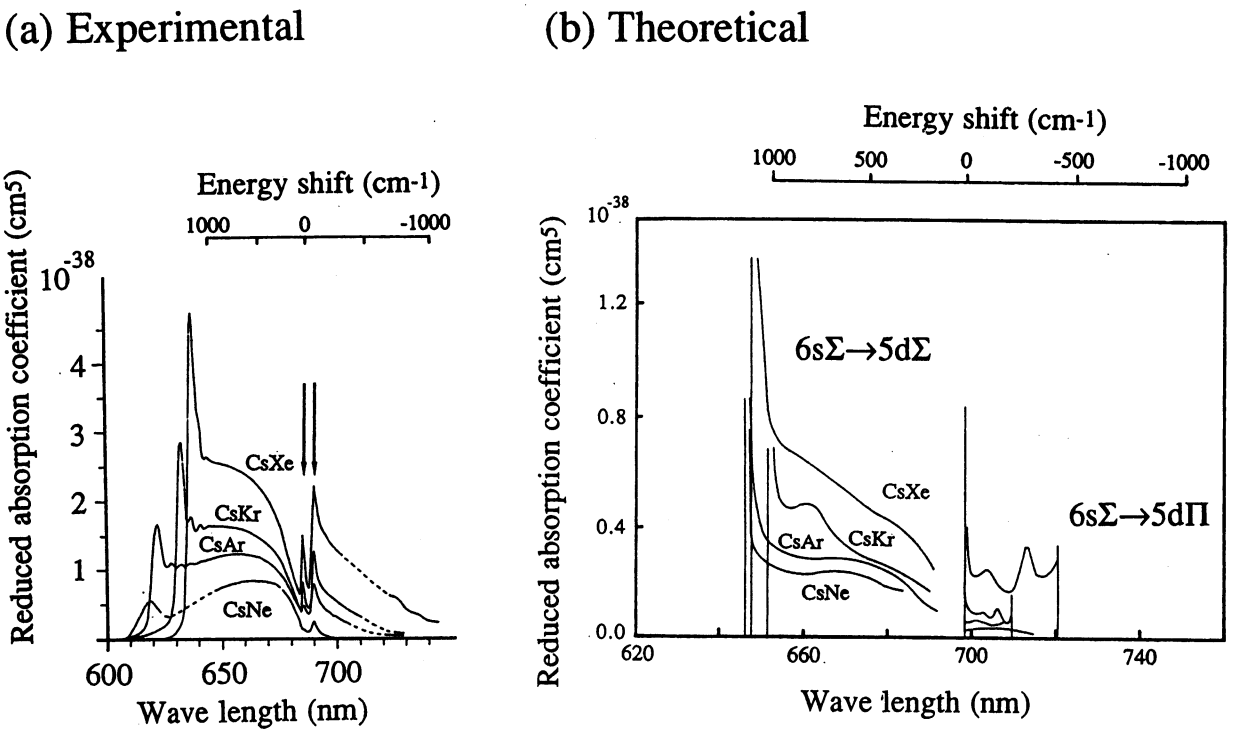

FIG. 8. (a) Experimental and (b) theoretical collision induced absorption spectra for the 5*d* state of the Cs–Rg system. Experimental spectra are cited from Ref. 2.

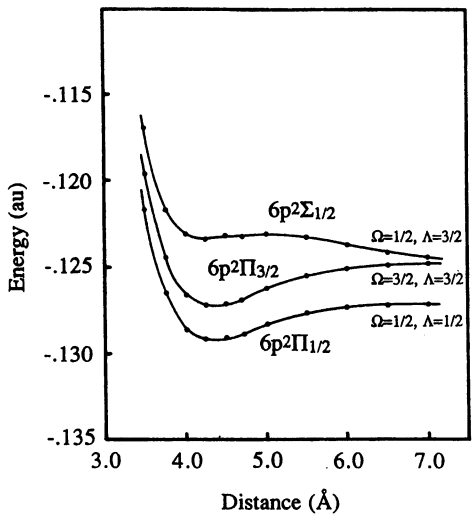

FIG. 9. Potential energy curves for the $6p^2\Sigma_{1/2}$, $6p^2\Pi_{3/2}$, and $6p^2\Pi_{1/2}$ states of the CsXe system calculated including the spin–orbit effects.

$6s\Sigma-6p^2\Sigma_{1/2}$ transitions of the CsRg system are summarized in Table V. The energy shifts are calculated to be about 400 cm^{-1}, while the observed ones are around 200 cm^{-1}.

The blue shift values for the $6s\Sigma-5d\Sigma$ transition shown in Table IV, are calculated to be larger than those for the $6s\Sigma-6p\Sigma$ ones for all the systems, as observed in the experimental spectra.[2,5] This is due to the fact that the $5d\Sigma$ state is more repulsive than the $6p\Sigma$ state.

The $6p^2\Pi_{1/2}$ and $6p^2\Pi_{3/2}$ states are responsible for the red bands and their band intensities gradually fall off away from the $6S-6P$ atomic line. However, the calculated emission bands in the red wing have small spikes which are due to the Boltzmann distributions in the upper bound states. These spikes are less clear in the experimental spectra, though they seem to be observed for the Kr and Ar complexes.

VII. SUMMARY

We have applied the SAC-CI method to the calculations of the collision induced absorption spectra of the CsRg sys-

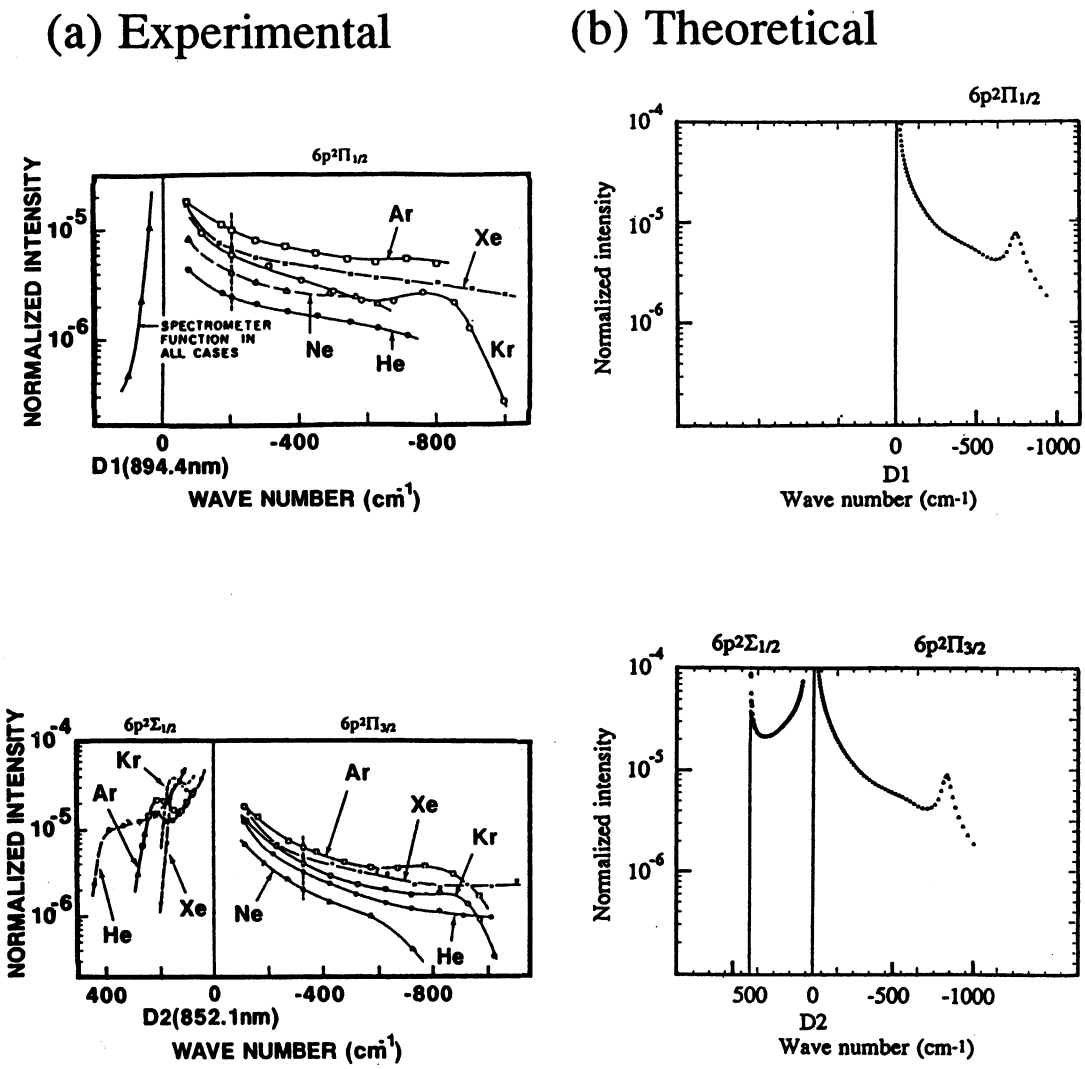

FIG. 10. (a) Experimental and (b) theoretical emission spectra for the $6S\rightarrow6P$ transition of the CsXe system. Experimental spectra are cited from Ref. 5.

TABLE V. Energy shift of the $6s\Sigma-6p^2\Sigma_{1/2}$ transition relative to the $6S-6P$ transition of the Cs atom.

System	Expt. (cm^{-1})[a]	SAC-CI[b]	
		Shift (cm^{-1})	Internuclear distance (Å)
CsXe	~150	400	~5.00
CsKr	~150	350	~4.75
CsAr	~200	430	~4.50
CsNe	~230	420	~4.00

[a]Reference 5.
[b]Energy shift is estimated from the extremum of the difference potential.

tem (Rg=Xe, Kr, Ar, and Ne) associated to the $5D$ and $7S$ lines of the Cs atom. The broadening of the $6P$ resonance line is also investigated by the present method. The reduced absorption coefficient of the induced transition and the normalized intensity, which are directly observed by the experiment, are calculated using the quasistatic approximation. The spectroscopic constants for the bound states of this system are also calculated.

The relative positions and the avoided crossing interactions between the $5d\Sigma$ and $7s\Sigma$ states are important for the descriptions of the collision induced absorptions around the $5D$ and $7S$ forbidden lines. The monotonic shift of the spectral peaks with substituting the rare gas atom is confirmed to be due to the shift of this avoided crossing points. The direction and the magnitude of the calculated band shifts agree well with the experimental data.

The intensities of the $6s\Sigma-5d\Sigma$ transitions are calculated to be larger than those of the $6s\Sigma-7s\Sigma$ ones, which is attributed to the fact that the former transitions are induced in larger internuclear distances than the latter ones. The absorption intensities are calculated to decrease as the rare gas atom is substituted from Xe to Ne in accordance with the feature of the observed spectra.

ACKNOWLEDGMENTS

The calculations have been carried out using the HITAC M-680H at the computer center of the Institute for Molecular Science. This study has partially been supported by the Grant-in-Aid for Scientific research from the Japanese Ministry of Education, Science, and Culture.

[1] P. R. Brooks, Chem. Rev. **88**, 407 (1988).
[2] G. Moe, A. C. Tam, and W. Happer, Phy. Rev. A **14**, 349 (1976).
[3] A. C. Tam, G. Moe, B. R. Bulos, and W. Happer, Opt. Commun. **16**, 376 (1976).
[4] A. C. Tam, G. Moe, W. Park, and W. Happer, Phys. Rev. Lett. **35**, 85 (1975).
[5] R. E. Hedges, D. L. Drummond, and Alan Gallagher, Phys. Rev. A **6**, 1519 (1972).
[6] J. F. Kielkopf and N. F. Allard, J. Phys. B **13**, 709 (1980); Rev. Mod. Phys. **54**, 1103 (1982).
[7] W. E. Baylis, J. Chem. Phys. **51**, 2665 (1969).
[8] J. Pascale and J. Vandeplanque, J. Chem. Phys. **60**, 2278 (1974).
[9] J. Pascale, J. Chem. Phys. **67**, 204 (1977).
[10] B. Sayer, J. P. Visticot, and J. Pascale, J. Phys. (Paris) **39**, 361 (1978).
[11] H. Nakatsuji and M. Ehara, Chem. Phys. Lett. **172**, 261 (1990).
[12] P. D. Kleiber and K. M. Sando, Phys. Rev. A **35**, 3175 (1987).
[13] P. D. Kleiber, A. K. Fletcher, and K. M. Sando, Phys. Rev. A **37**, 3584 (1988).
[14] K. Ueda, T. Komatsu, and Y. Sato, J. Chem. Phys. **91**, 4495, 4499 (1989); K. Ueda, H. Sotome, and Y. Sato, *ibid.* **94**, 1903, 1907 (1991); K. Ueda, O. Sonobe, H. Chiba, and Y. Sato, *ibid.* **95**, 8083 (1991); T. Maeyama, H. Ito, H. Chiba, K. Ohmori, K. Ueda, and Y. Sato, *ibid.* **97**, 9492 (1992).
[15] K. Ohmori, T. Kurosawa, H. Chiba, M. Okunishi, and Y. Sato, J. Chem. Phys. **100**, 5381 (1994).
[16] H. Nakatsuji and K. Hirao, J. Chem. Phys. **68**, 2053 (1978).
[17] H. Nakatsuji, Chem. Phys. Lett. **59**, 362 (1978); **67**, 329, 334 (1979).
[18] H. Nakatsuji, Acta Chim. Hungarica **129**, 719 (1992).
[19] H. Nakatsuji, J. Ushio, and T. Yonezawa, Can. J. Chem. **63**, 1857 (1985).
[20] Y. Mizukami and H. Nakatsuji, J. Chem. Phys. **92**, 6084 (1990).
[21] J. Holmtzmark, Ann. Phys. (Leipzig) **58**, 577 (1919).
[22] A. Jablonski, Phys. Rev. **68**, 78 (1945).
[23] S. Y. Chen and M. Takeo, Rev. Mod. Phys. **29**, 20 (1957).
[24] W. R. Wadt and P. J. Hay, J. Chem. Phys. **82**, 284 (1985).
[25] S. R. Langhoff, C. W. Bauschlicher, and H. Partrige, J. Phys. B **18**, 13 (1985).
[26] S. Huzinaga, J. Andzelm, M. Klobukowski, E. Radzio-Andzelm, Y. Sakai, and H. Tatewaki, *Gaussian Basis Sets for Molecular Calculations* (Elsevier, Amsterdam, 1984).
[27] W. C. Ermler, Y. S. Lee, K. S. Pitzer, and N. W. Winter, J. Chem. Phys. **69**, 716 (1971).
[28] H. Nakatsuji, Chem. Phys. **75**, 425 (1983).
[29] M. Dupuis, J. D. Watts, H. O. Viller, and G. J. B. Hurst, Program System HONDO7, Program Library No. 544, Computer Center of the Institute for Molecular Science, 1989.
[30] H. Nakatsuji, Program system for SAC and SAC-CI calculations, Program Library No. 146 (Y4/SAC), Data Processing Center of Kyoto University, 1985; H. Nakatsuji, Program Library SAC85 (No. 1396), Computer Center of the Institute for Molecular Science, Okazaki, Japan, 1986.
[31] (a) H. Nakatsuji, Y. Matsuzaki, and T. Yonezawa, J. Chem. Phys. **88**, 5759 (1988); (b) C. A. Masmanidis, H. H. Jaffe, and R. L. Ellis, J. Phys. Chem. **79**, 2052 (1975); (c) S. Kato, R. L. Jaffe, A. Komornicki, and K. Morokuma, J. Chem. Phys. **78**, 4567 (1983).
[32] C. E. Moore, *Atomic Energy Levels* (National Bureau of Standards, Washington, D. C., 1971), Vol. 2.
[33] G. Alber and J. Cooper, Phys. Rev. A **33**, 3084 (1986).
[34] U. Buck and H. Pauly, Z. Phys. **208**, 390 (1968).
[35] Q. Ma and R. H. Tipping, J. Chem. Phys. **95**, 6290 (1991); **96**, 8655 (1992); **97**, 818 (1992); **100**, 2537 (1994).